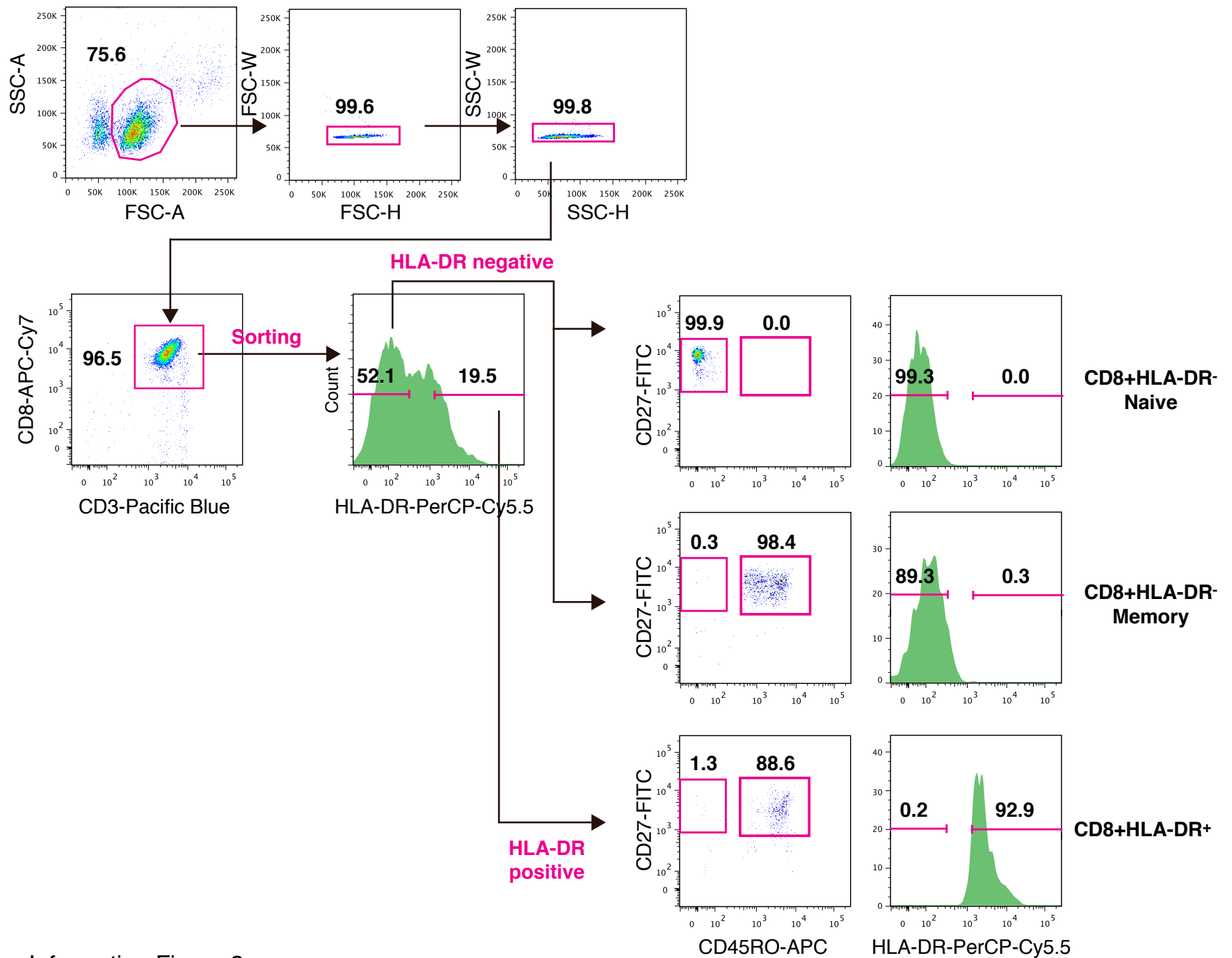


Supporting Information Fig.1

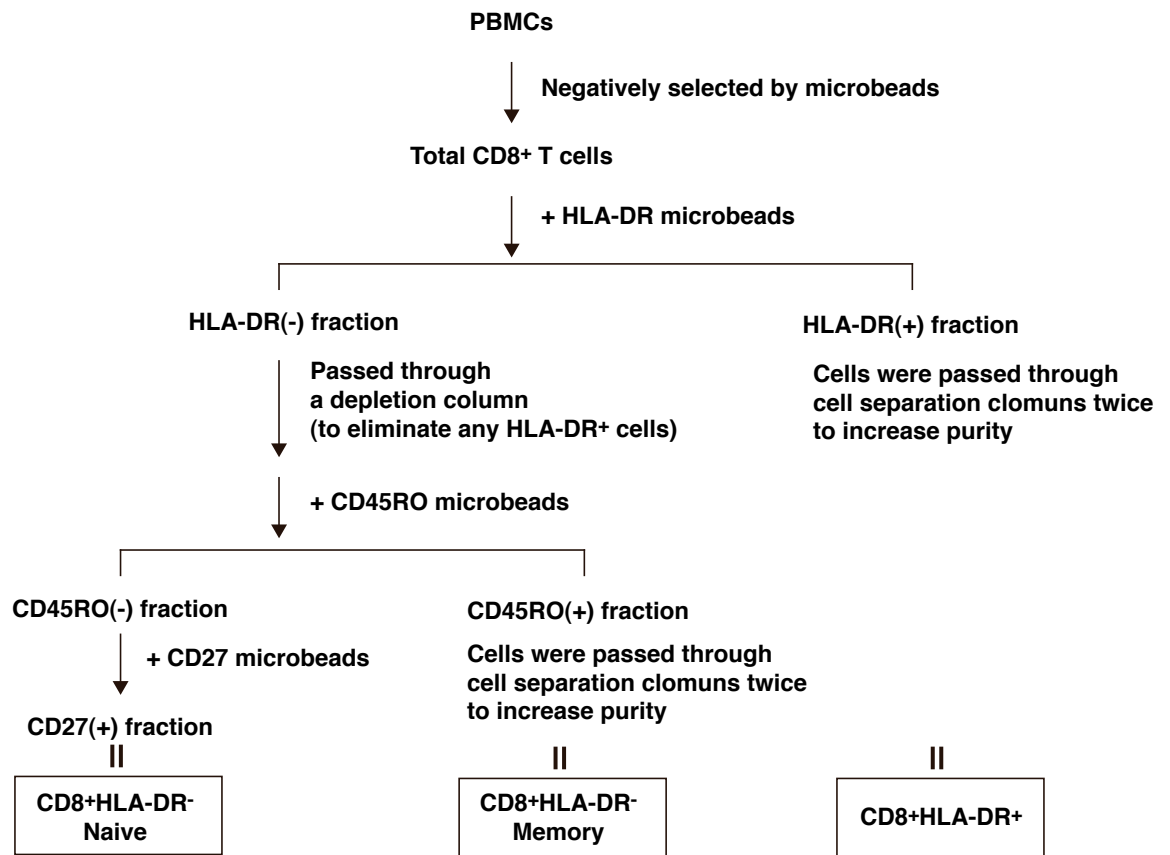
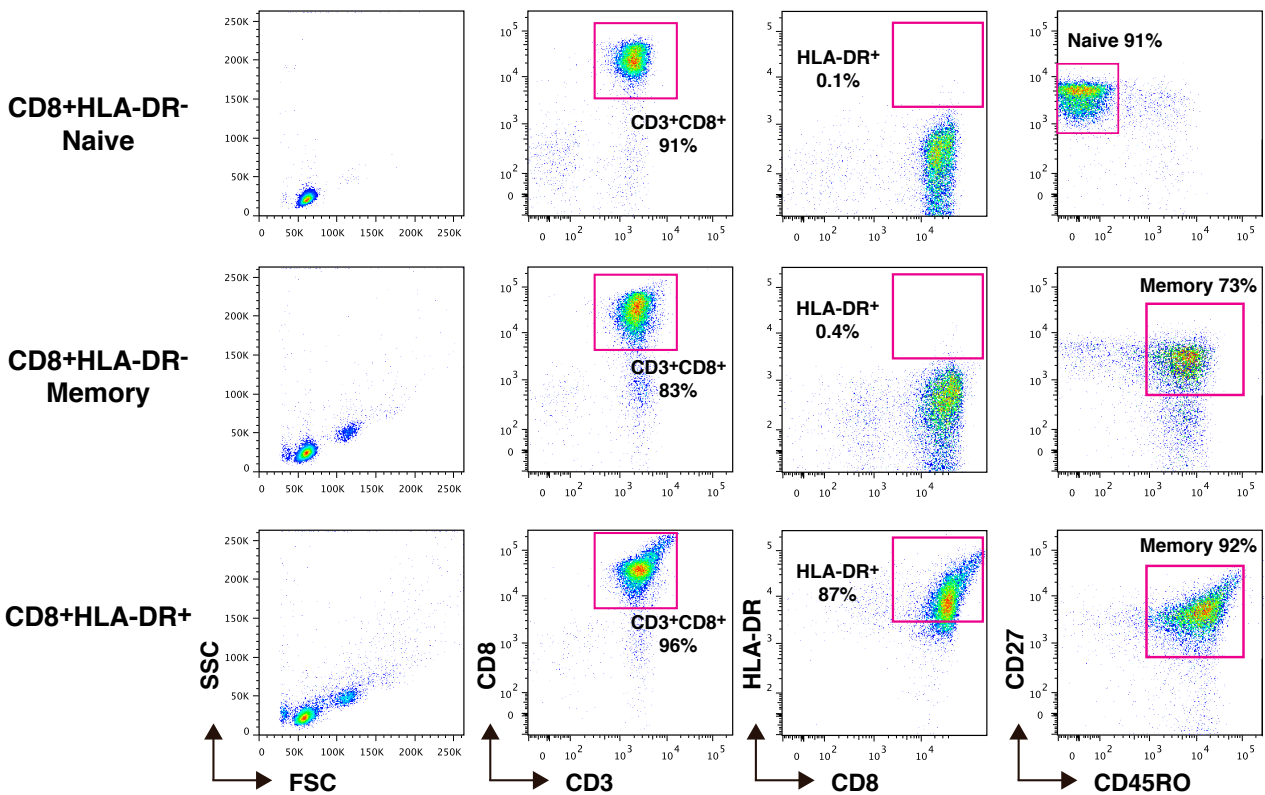
Distribution of naive and memory phenotypes within CD8⁺HLA-DR⁻ and CD8⁺HLA-DR⁺ T cells. Naive cells are defined as CD45RO⁻CD27⁺; and memory cells are defined as CD45RO⁺CD27⁺, as indicated in the plots. Two different patterns representing the donor from 10 healthy controls are shown.

Enriched CD8+ T cells



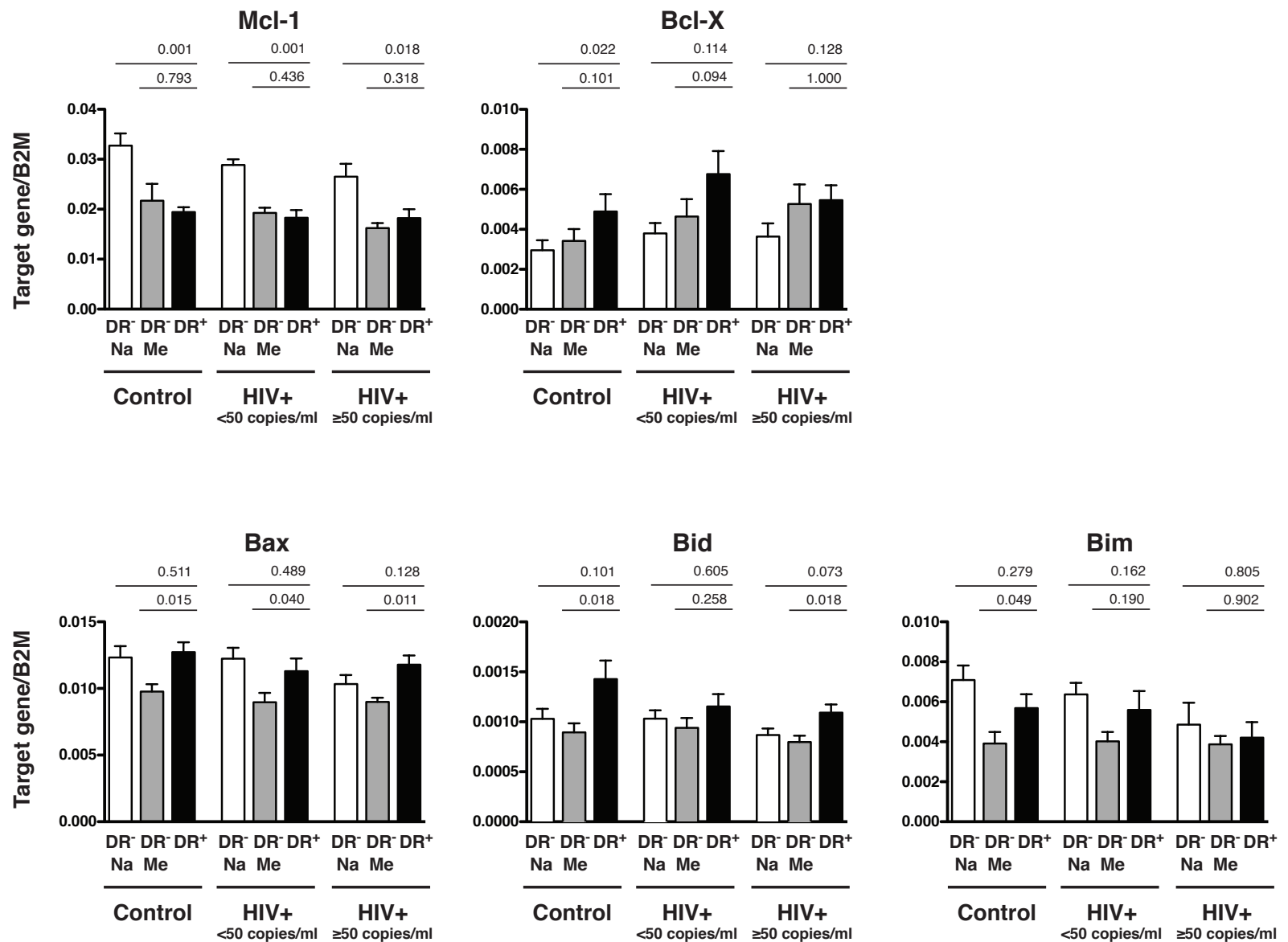
Supporting Information Figure 2

Gating strategy used for FACS sorting of CD8+HLA-DR- naive, CD8+HLA-DR- memory and CD8+HLA-DR+ subsets for studies depicted in Figures 4, 7 and 8.

A**B**

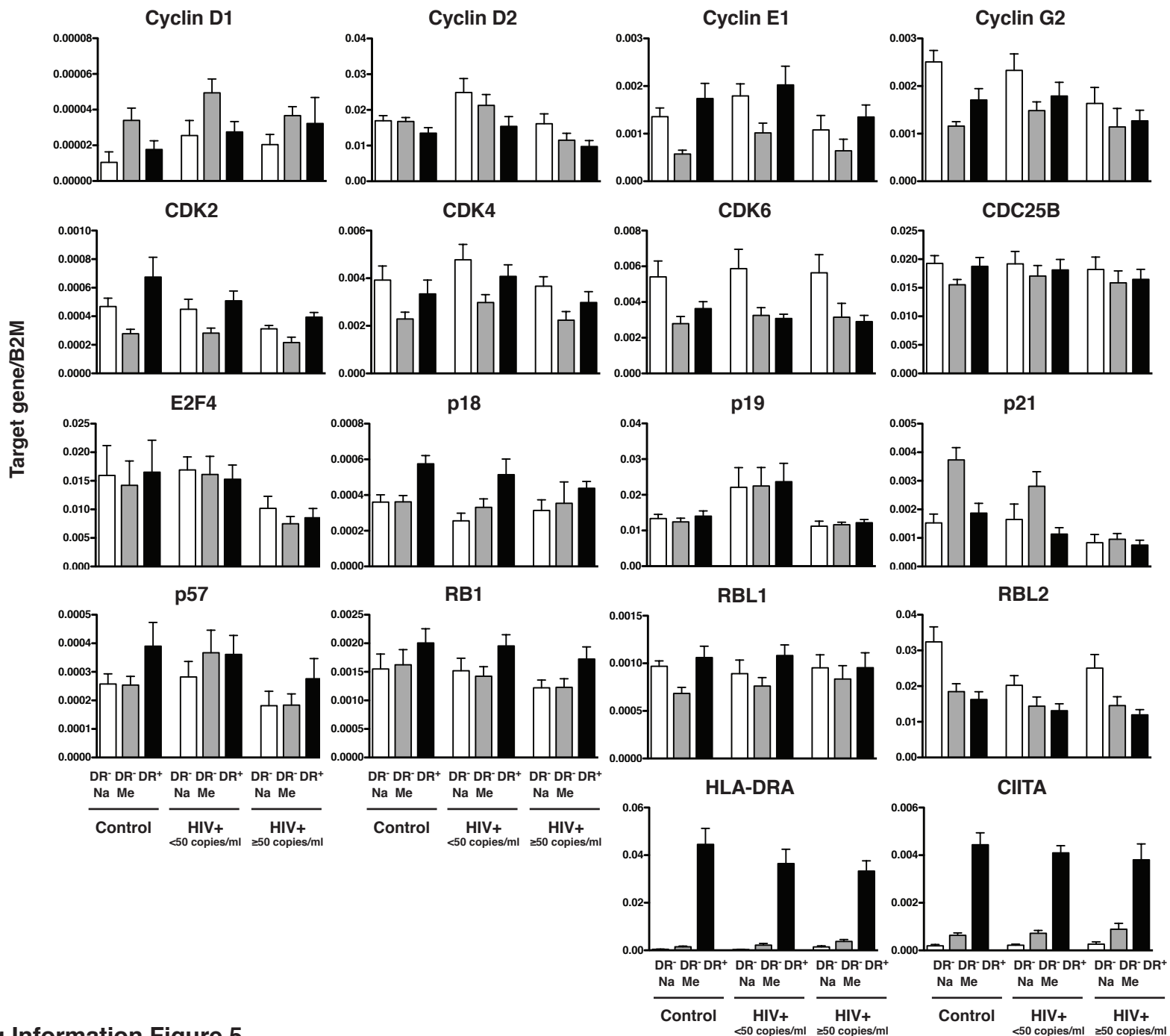
Supporting Information Figure 3

Purification of CD8+HLA-DR⁻ naive, CD8+HLA-DR⁻ memory and CD8+HLA-DR⁺ T cell subsets by magnetic microbeads. (A) A schematic diagram depicting the strategy used to obtain pure populations of CD8+HLA-DR⁻ naive, CD8+HLA-DR⁻ memory and CD8+HLA-DR⁺ T cells from PBMCs by magnetic beads. (B) The purity of the cells was assessed following separation by staining the cells with anti-CD3, CD8, HLA-DR, CD45RO and CD27 antibodies by flow cytometry.



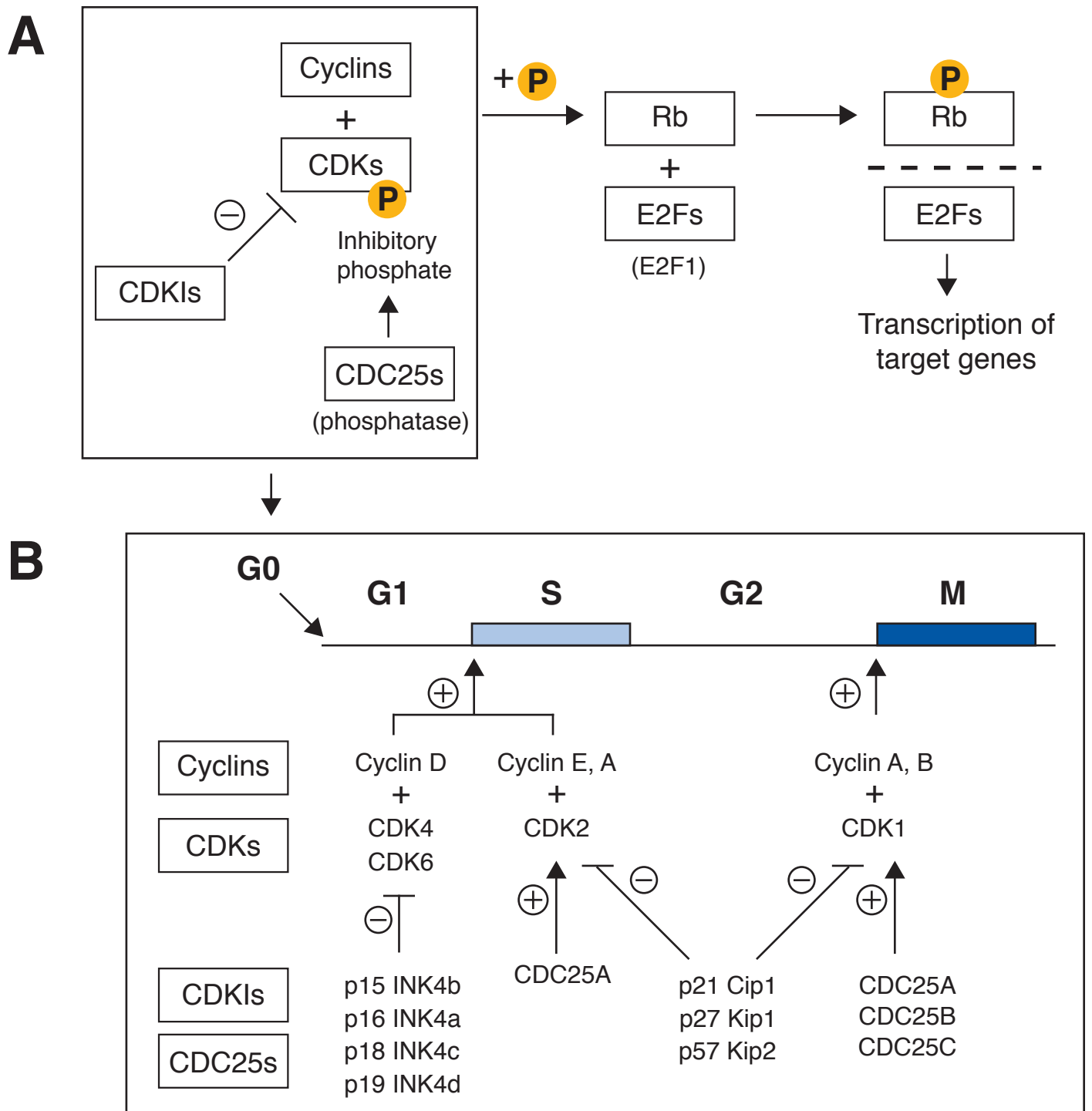
Supporting Information Figure 4

Expression levels of anti-apoptotic (Mcl-1, Bcl-X) and pro-apoptotic (Bax, Bid and Bim) genes. Mean±SEM values were calculated from FACS-sorted CD8⁺HLA-DR⁻ naive, CD8⁺HLA-DR⁻ memory and CD8⁺HLA-DR⁺ T cells from control (n=11), HIV+ <50 (n=9) and HIV+ ≥50 (n=7) individuals. DR⁻ and DR⁺ stand for HLA-DR negative and HLA-DR positive cells, respectively. Na and Me stand for naive and memory cells, respectively. The level of statistical significance was determined by the Mann-Whitney nonparametric test.



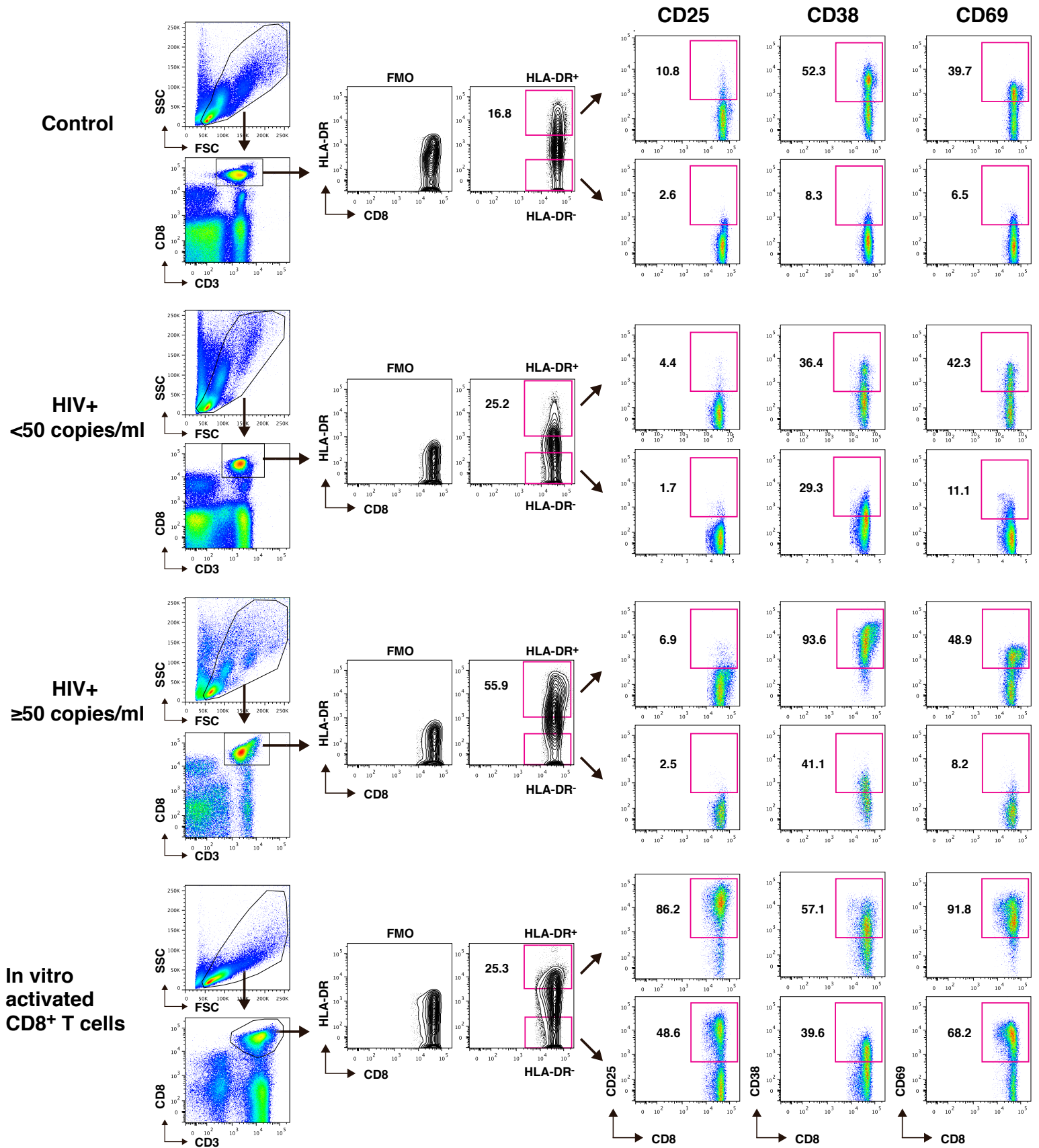
Supporting Information Figure 5

Expression of additional 16 genes involved in cell cycle and signature (HLA-DR and CIITA) genes in FACS-sorted CD8⁺HLA-DR⁻ naive, CD8⁺HLA-DR⁻ memory and CD8⁺HLA-DR⁺ T cells. Mean±SEM values were calculated from control (n=9), HIV+ <50 (n=10) and HIV+ ≥50 (n=9) individuals. DR⁻ and DR⁺ stand for HLA-DR negative and HLA-DR positive cells, respectively. Na and Me stand for naive and memory cells, respectively. Expression of cyclin A1 and p16 INK4b was not detected with 40 cycles of PCR amplification.



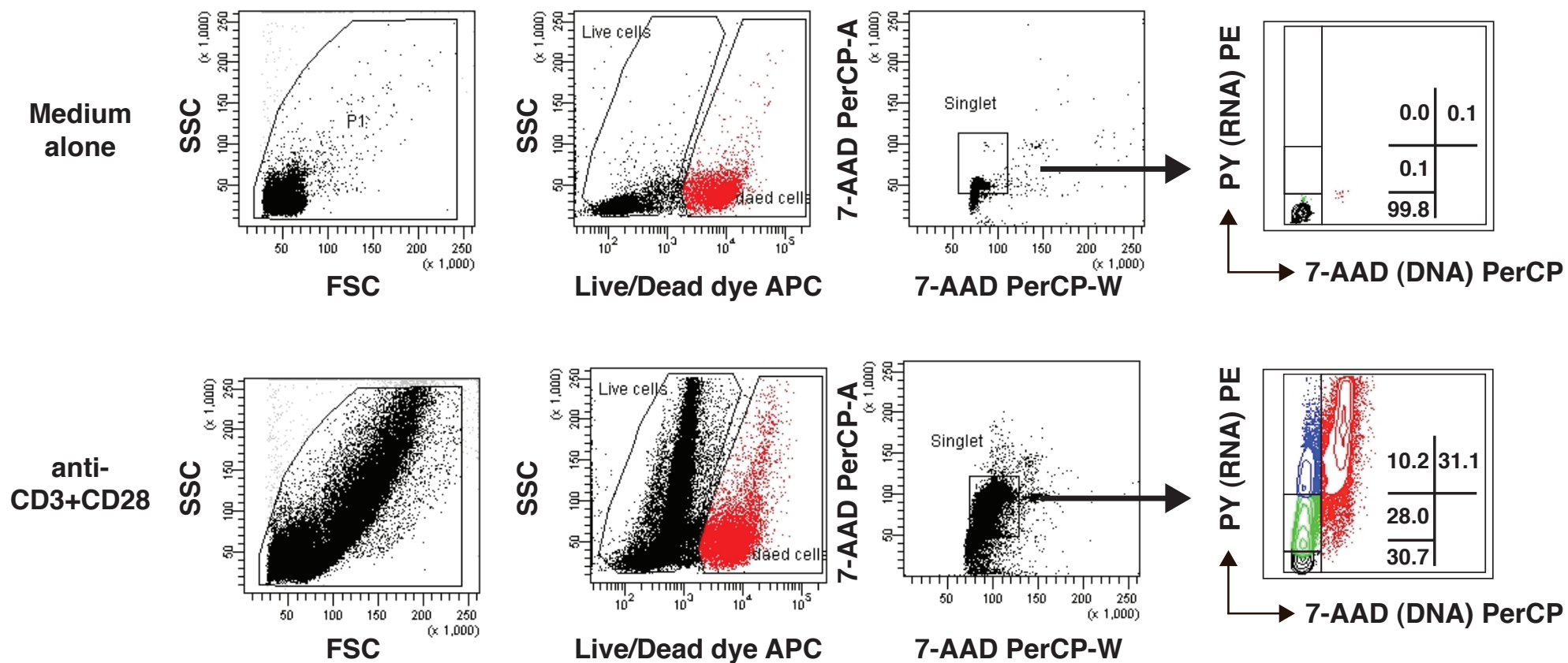
Supporting Information Figure 6.
Schematic diagram of control of cell cycle progression.

A, Entry of quiescent (G0) cells into G1 phase of cell cycle involves induction of a number of cell cycle activators, including D-type cyclins and cyclin-dependent kinases (CDKs) 4/6. Activation of cyclin D-CDK4/6, in conjunction with subsequent activation of cyclin E-CDK2, results in phosphorylation of members of the retinoblastoma protein family (Rb). Hyperphosphorylated Rb dissociates from the E2F transcription factor family members (E2Fs), allowing the transcription of several genes required progression through G1 phase of the cell cycle. **B**, Mammalian CDKs are negatively regulated by CDK inhibitors. Members of the INK4 family (p16 INK4a, p15 INK4b, p18 INK4c, and p19 INK4d) specifically inactivate CDK4 and CDK6, whereas members of the CIP/KIP family (p21 CIP1, p27 KIP1, and p57 KIP2) inhibit activity of all CDKs by forming a ternary complex with cyclin-CDK. A family of dual-specificity phosphatases, CDC25s, activates both CDK1 and CDK2 by dephosphorylating inhibitory phosphates: Tyr15 and Thr14. Among the three known isoforms: CDC25A, B and C, CDC25A promotes entry into S phase by acting on cyclinE-CDK2 and cyclin A-CDK2, whereas CDC25B and CDC25C play a role in the onset of mitosis.



Supporting Information Figure 7

Representative plots of cell surface expression of CD25, CD38 and CD69 on CD8+HLA-DR- and CD8+HLA-DR+ T cells from control (n=14), HIV+ <50 copies/ml (n=17), HIV+ ≥50 copies/ml (n=9) individuals and in vitro activated CD8+ T cells (n=3).



Supporting Information Figure 8

Gating strategy used to analyze cell cycle status by 3-color flow cytometry. Plots are one representative set from CD8⁺HLA-DR⁻ naive cells that were cultured with medium alone or anti-CD3+CD28 for 2 days. The data are from the same HIV-infected individual (HIV-RNA <50 copies/ml) used for the analysis shown in Figure 6.

Supporting Information Table 1. TaqMan Primer/Probe sets used in the study.

1.	B2M	Hs99999907_m1	
2.	CCNA1	Hs00171105_m1	cyclin A1
3.	CCNA2	Hs00153138_m1	cyclin A2
4.	CCND1	Hs00277039_m1	cyclin D1
5.	CCND2	Hs00277041_m1	cyclin D2
6.	CCND3	Hs00426901_m1	cyclin D3
7.	CCNE1	Hs00233356_m1	cyclin E1
8.	CCNB1	Hs00259126_m1	cyclin B1
9.	CCNG2	Hs00171119_m1	cyclin G2
10.	CDK1	Hs00938778_m1	
11.	CDK2	Hs00608082_m1	
12.	CDK4	Hs00364847_m1	
13.	CDK6	Hs01026372_m1	
14.	RB1	Hs00153108_m1	
15.	RBL1	Hs00161234_m1	Rb p107
16.	RBL2	Hs00180562_m1	Rb p130
17.	CDKN2B	Hs00394703_m1	p15 INK4b
18.	CDKN2A	Hs00233365_m1	p16 INK4a
19.	CDKN2C	Hs00176227_m1	p18 INK4c
20.	CDKN2D	Hs00176481_m1	p19 INK4d
21.	CDKN1A	Hs99999142_m1	p21 Cip1
22.	CDKN1B	Hs00153277_m1	p27 Kip1
23.	CDKN1C	Hs00175938_m1	p57 Kip2
24.	CDC25A	Hs00153168_m1	
25.	CDC25B	Hs00244740_m1	
26.	CDC25C	Hs00156411_m1	
27.	E2F1	Hs00153451_m1	
28.	E2F4	Hs00608098_m1	
29.	CIITA	Hs00172106_m1	
30.	HLA-DRA	Hs00219578_m1	
31.	CDC6	Hs00154374_m1	
32.	CDT1	Hs00417193_g1	
33.	BAX	Hs01016552_g1	Bax
34.	BID	Hs00609632_m1	Bid
35.	BIM	Hs00708019_m1	BCL2L11
36.	BCL2	Hs00153350_m1	Bcl-2
37.	MCL1	Hs00172036_m1	Mcl-1
38.	BIRC5	Hs00153353_m1	Survivin

Beta-2 microglobullin (*B2M*) was used for normalization

Supporting Information Table 2. Antibodies used in the western blot.

1. Cyclin D3 (2936; Cell Signaling)
2. Cyclin A (05-374; Millipore)
3. Cyclin B1 (05-373; Millipore)
4. Cdc2 (CDK1) (06-923; Millipore),
5. p16 INK4a (sc-467; Santa Cruz),
6. p27 Kip1 (06-445; Millipore)
7. CDC25A (05-743; Millipore)
8. CDC25C (05-507; Millipore)
9. E2F1 (05-379; Millipore)
10. Cdc6 (sc-9964; Santa Cruz)
11. CDT1 (TA305481; Origene)
12. Bcl-2 (2872; Cell Signaling)
13. Survivn (2802; Cell Signaling)
14. beta-Actin (ab8226; Abcam) for the assessment of loading equivalency of whole cell lysate
15. TFII-I antibody (4562; Cell Signaling) for the assessment of loading equivalency of nuclear extract.